REPORT DOCUMENTATION PAGE

Form Approved OMB No. 0704-0188

1. REPORT DATE *(DD-MM-YYYY)*	2. REPORT TYPE	3. DATES COVERED *(From – To)*
05-01-2006	Final Report	1 October 2002 - 26-Jun-06

4. TITLE AND SUBTITLE

Study of Experimental Aspects of Dynamic Modeling and Control System Analysis of Hovering Flights of Eristalis Hoverflies

5a. CONTRACT NUMBER
F61775-02-C4048

5b. GRANT NUMBER

5c. PROGRAM ELEMENT NUMBER

6. AUTHOR(S)

Dr. Rafal W Zbikowski

5d. PROJECT NUMBER

5d. TASK NUMBER

5e. WORK UNIT NUMBER

7. PERFORMING ORGANIZATION NAME(S) AND ADDRESS(ES)

Cranfield University
RMCS Shrivenham
Swindon SN6 8LA
United Kingdom

8. PERFORMING ORGANIZATION REPORT NUMBER
N/A

9. SPONSORING/MONITORING AGENCY NAME(S) AND ADDRESS(ES)

EOARD
PSC 821 BOX 14
FPO 09421-0014

10. SPONSOR/MONITOR'S ACRONYM(S)

11. SPONSOR/MONITOR'S REPORT NUMBER(S)
SPC 02-4048

12. DISTRIBUTION/AVAILABILITY STATEMENT

Approved for public release; distribution is unlimited.

13. SUPPLEMENTARY NOTES

14. ABSTRACT

This report results from a contract tasking Cranfield University as follows: The contractor will investigate and develop mathematical models, with predictive capabilities, of Eristalis hoverfly flight stability & control systems.
Eristalis hoverflies have wing-beat frequency that is an order of magnitude higher than that of the desert locust (ca. 150Hz vs ca. 20 Hz). The frequency response necessary to characterize the frequency components of the flight forces and moments that impact on flight dynamics needed to be determined. By recording hovering Eristalis hoverflies using 4 high-speed digital cameras recording at 4000fps, it was verified that the time-specific forcing of the wingbeat is not manifested strongly in the body dynamics, as oscillations of the body at the wingbeat frequency are scarcely discernible, even in video of sufficient resolution to resolve individual hairs on the fly's abdomen. This implies that it may not be necessary to formulate the full time-periodic equations of motion in order to model the flight dynamics of Eristalis hoverflies realistically. This is in contrast to the situation for the larger desert locust, whose larger size and longer time constants mean that a time-periodic model is essential. Thus, it follows that if we can record the fundamental frequency of the hoverfly wingbeat faithfully using our force balance, we may be confident that the frequency response of the balance is adequate to model hoverfly flight dynamics. The frequency response of the balance is almost 600Hz with a hoverfly attached, and this should therefore be more than sufficient to measure reliably force components at the fundamental frequency of the wingbeat. One of the key goals of the study was to develop a new apparatus suitable for deriving dynamics models for any large insect, including desert locusts and Eristalis hoverflies. A detailed description of the various components of the system will be published as a methods paper in biomechanics/neurophysiology literature.

15. SUBJECT TERMS

EOARD, Flight Mechanics, Aerodynamics

16. SECURITY CLASSIFICATION OF:			17. LIMITATION OF ABSTRACT	18, NUMBER OF PAGES	19a. NAME OF RESPONSIBLE PERSON
a. REPORT	b. ABSTRACT	c. THIS PAGE			ROBERT N. KANG, Lt Col, USAF
UNCLAS	UNCLAS	UNCLAS	UL	23	19b. TELEPHONE NUMBER *(Include area code)* +44 (0)20 7514 4437

Study of Experimental Aspects of Dynamic Modelling and Control System Analysis of Hovering Flight of *Eristalis* Hoverflies
FINAL REPORT

Rafał Żbikowski (Cranfield University, Defence Academy Shrivenham)

Richard J. Bomphrey, Jochem 't Hoen, Adrian L. R. Thomas
Simon M. Walker and Graham K. Taylor, (Oxford University, Zoology Department)

November, 2005

Contents

1 Introduction

This is the final report for the project under Contract No. F61775-02-C4048. The main motivation for the project was to explore suitable theoretical and experimental approaches to characterise flight dynamics and control of insects, originally focussing on the hovering flight of *Eristalis* hoverflies. The study was soon re-scoped to investigate the desert locust *Schistocerca gregaria*. Although the locust is an interesting insect in its own right, there were two main motivations for this change of focus. Firstly, it proved prudent from the experimental viewpoint to work with the larger and more robust locust, thus allowing us to perfect the experimental set-up and techniques before proceeding to the smaller hoverflies. Secondly, although forward flight was not originally envisaged as forming part of the study, it quickly became apparent that the greatest difficulties in experimentation were those associated with forward flight, not hover. Simulating forward flight poses such a significant challenge—but is so important to reverse engineering insect flight control—that we elected to develop from the outset a system capable of simulating natural forward flight. This approach has thus allowed us not only to re-focus, but also to broaden the study.

Investigating the flight dynamics and control of insects, as opposed to manmade vehicles, poses its own unique problems, limiting applicability of a large body of the relevant aeronautical knowledge. The first and foremost difficulties are experimental in nature, exacerbated by the fact that insects are small and fragile. However, the key issue is that neither wind tunnel, nor free flight, testing can be done satisfactorily with the present state-of-the-art, especially from the point of view of meaningful aerodynamic force and moment measurement. In standard aeronautical wind tunnel testing, a model is mounted on a force balance which, in turn, is placed on a moving platform, thus allowing direct force and moment measurement, while controlling the model's orientation with respect to the tunnel's airflow. There are two difficulties with this standard aeronautical set-up in the context of insect flight. Firstly, one cannot make a distinction between the pilot and the airframe—the insect flight control system cannot be switched off to investigate open-loop dynamics. Secondly, insect flight behaviour is influenced by many of its sensory modalities, including vision, and it is difficult to provide artificial stimulation that faithfully reproduces all forms of natural excitation at the same time. In free flight testing the second difficulty is mitigated, but at the price of losing the possibility of direct force/moment measurement.

These experimental challenges have counter-intuitive consequences for theoretical analysis. It is not unreasonable to represent the insect flight dynamics by the standard six-degrees-of-freedom (6dof) equations of motion, so the fundamental question is then: "What do these equations represent?" Since it is impossible to switch off the insect's flight control system, the conventional approach of deriving the open-loop dynamics, then postulating a feedback control law and closing the loop is unfeasible. Moreover, unless all of the sensory modalities are artificially stimulated in a manner consistent with natural flight, the insect's control system may be confused. Indeed, the animal will beat its wings as it would normally do in free flight, but some of the expected flight dynamic effects will not be detected by the sensors. Hence, the physiologically intact muscles-wings-sensors loop is broken by the constraints of the experiments and what is observed is neither open- nor closed-loop dynamics, but what

we term “broken dynamics” [1]. Therefore, the central question is how meaningful it is to input the measurements of the experiments to the 6dof equations of motion. It is likely that within the limitations of the experimental set-up available in this project, we saw various aspects of broken dynamics.

If what was observed was indeed broken dynamics, how useful was the exercise? There are two important advantages of this work: 1) real-life application of both theoretical and experimental tools of advanced flight dynamics for insects, 2) lessons learnt from 1 suggesting ways of overcoming the limitations of the set-up used. This report focusses largely on 1, commenting in Section 3 on 2.

This document is structured as follows. Section 2 covers theoretical developments, while Section 3 focusses on the experimental work. Due to the abundance of mathematical modelling tools, and the experimental difficulties described above, it is easy to propose a variety of mathematical models, but it is much more challenging to support the models with realisable experiments. In this context, we consider the non-linear time periodic modelling (NLTP) framework as an appropriate combination of theory and experiment and a major contribution of this project. The details of the approach and its results are described in a reprint of our paper [1] which constitutes an appendix to this report. The body of Section 2 presents other theoretical ideas generated in the project, but not realised due to the limited resources and/or limitations of the experimental state-of-the-art. The body of Section 3 presents advances in the experimental techniques which go beyond the set-up described in [1] and the concomitant results.

2 Theoretical work

This section presents theoretical developments generated during the project which could not yet be accompanied by in-depth experimental work due to the limited resources and/or limitations of the experimental state-of-the-art. We begin with the basics of flight dynamics in the context of insect flight in Section 2.1. This is followed by a short exposition of external (Section 2.2) and internal (Section 2.3) modelling. This framework is independent of the NLTP model [1], but can be applied in the NLTP context. By contrast, the mathematical tools described in Sections 2.4 to 2.6 were identified as specialised techniques relevant to the NLTP modelling framework.

2.1 Basics

Flight dynamics arise because the insect trajectory cannot change instantaneously in response to the aerodynamic force and moment generated by flapping wings. This is due to complex interactions of the inertia of the insect’s body with the airflow around the body. Assuming that the body is rigid and longitudinally symmetric, the interactions are quantified by the equations of motion [2], [3]:

$$m(\dot{u} - vr + wq) = mg_x + X \quad (1)$$

$$m(\dot{v} + ur - wp) = mg_y + Y \quad (2)$$

$$m(\dot{w} - uq + vp) = mg_z + Z \quad (3)$$

$$I_{xx}\dot{p} + (I_{zz} - I_{yy})qr - I_{xz}(\dot{r} + pq) = L \quad (4)$$

$$I_{yy}\dot{q} - (I_{zz} - I_{xx})pr + I_{xz}(p^2 - r^2) = M \quad (5)$$

$$I_{zz}\dot{r} + (I_{yy} - I_{xx})pq - I_{xz}(\dot{p} - qr) = N. \quad (6)$$

For an insect of mass m and inertia tensor $\boldsymbol{I}$ the coordinate system is fixed to its body at the centre of gravity, see Figure 1. The translational velocity is $\boldsymbol{V} = (u, v, w)$ and the angular velocity $\boldsymbol{\omega} = (p, q, r)$. Also, the aerodynamic force $\boldsymbol{F} = (X, Y, Z)$, the aerodynamic moment $\boldsymbol{M} = (L, M, N)$, and the gravity vector is resolved as $\boldsymbol{g} = (g_x, g_y, g_z)$. Equations (1)–(6) can be rewritten in terms of the sideslip angle $\beta = \sin^{-1}(v/V)$ and the angle of attack $\alpha = \sin^{-1}(u/V\cos\beta)$, where $V = \sqrt{u^2 + v^2 + w^2}$ is the speed.

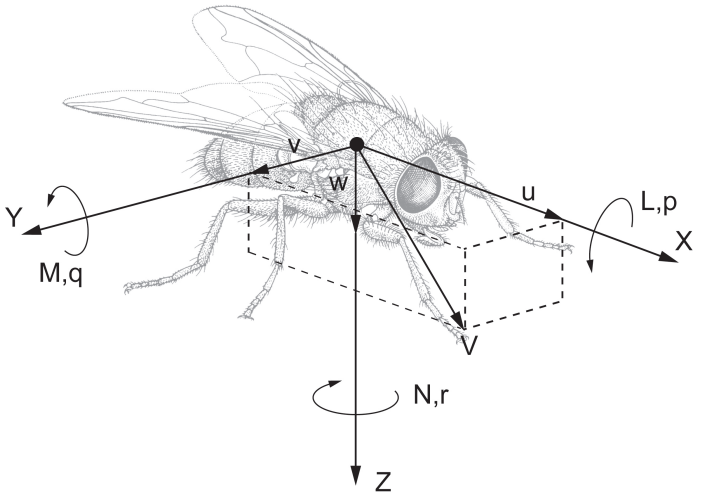

Figure 1: Coordinate system and notation for insect flight dynamics equations.

It is convenient to have a short-hand for (1)–(6) in the form:

$$\dot{\boldsymbol{x}} = \boldsymbol{f}_o(\boldsymbol{x}, \boldsymbol{u}) \quad (7)$$

with the state $\boldsymbol{x} = (u, v, w, p, q, r)$ and the control input $\boldsymbol{u} = (X, Y, Z, L, M, N)$. The key to successful flight is purposeful generation of the control input $\boldsymbol{u}$, i.e. aerodynamic force $\boldsymbol{F}$ and moment $\boldsymbol{M}$. The insect controls their production by modulating the flapping of its wings, comparing the actual and required trajectory, so that a feedback loop is formed to follow the required trajectory. Since in equation (7) the control $\boldsymbol{u}$ is not specified as a function of $\boldsymbol{x}$, i.e. the feedback loop has not been defined, it is called open-loop dynamics.

For piloted aircraft, the required trajectory $\boldsymbol{r}$ is known from the aircraft mission and/or flight manual. Similarly, the feedback law $\boldsymbol{\phi}$ is also known, as it was specified when the aircraft was designed. In a manoeuvre, aircraft flight dynamics arise from substituting $\boldsymbol{u}(t) = \boldsymbol{\phi}(\boldsymbol{r}(t), \boldsymbol{x}(t), t)$ in (7) to obtain the closed-loop dynamics:

$$\dot{\boldsymbol{x}} = \boldsymbol{f}_o(\boldsymbol{x}, \boldsymbol{u})|_{\boldsymbol{u}=\boldsymbol{\phi}(\boldsymbol{r},\boldsymbol{x},t)} = \boldsymbol{f}_c(\boldsymbol{x}, t). \quad (8)$$

The distinction between the "pilot" and the "aircraft" cannot be made for an insect, and the mission (or "flight manual") can only be speculated about. There is no possibility of asking the pilot (the insect itself) or the designer (natural selection) about the required trajectory $\boldsymbol{r}$ or the feedback law $\boldsymbol{\phi}$ used. Hence, the open-loop description (7) cannot be obtained experimentally. However, it may still be possible to deduce the closed-loop description $\boldsymbol{f}_c$ to gain conceptual, functional and physical insights into flight dynamics of free-flying, manoeuvrable insects. Subsequent deduction of $\boldsymbol{f}_o$ (and thus $\boldsymbol{r}$ and $\boldsymbol{\phi}$) from $\boldsymbol{f}_c$ is then a separate task.

2.2 External modelling: Bifurcation analysis

The purpose of external modelling is to derive a tractable mathematical description of free-flying, manoeuvrable insects which would be experimentally feasible, while capturing the nonlinear and time-varying complexity of the flight dynamics involved.

When the aerodynamic force and moment are balanced by the insect's weight, the insect will be in steady flight. Linearisation of equations (1)–(6) around the steady flight trajectory $\bar{\boldsymbol{x}}$ approximates (8) with

$$\delta\dot{\boldsymbol{x}} = \boldsymbol{A}_c\delta\boldsymbol{x}, \tag{9}$$

where the variable $\delta\boldsymbol{x} = \boldsymbol{x} - \bar{\boldsymbol{x}}$ is a perturbation of the trajectory $\bar{\boldsymbol{x}}$. For a constant trajectory, $\bar{\boldsymbol{x}}(t) \equiv \text{const}$, $\boldsymbol{A}_c$ is a constant matrix. If the steady flight is periodic, $\bar{\boldsymbol{x}}(t + T) = \bar{\boldsymbol{x}}(t)$, then the matrix is periodic (time-varying), $\boldsymbol{A}_c(t + T) = \boldsymbol{A}_c(t)$. Both cases are mathematically tractable [4].

In contrast to steady flight, manoeuvres entail the nonlinear, dynamic phenomena of: 1) inertial coupling [3], see equations (4)–(6), 2) aerodynamic cross-coupling [5], i.e. interdependence among the components of $\boldsymbol{F}$ and $\boldsymbol{M}$, and 3) unsteady aerodynamics [6]. Linearisation (9) simplifies away 1) and 2), but the effects of 3) can be included, albeit in an approximate fashion, as is now explained on the example of the pitching moment M.

The pitching moment M in (9) is assumed to depend linearly on the current value of the angle of attack α, i.e. $M(t) = M_\alpha\alpha(t)$, where M_α is a constant. In manoeuvre, the pitching moment will not change instantaneously in response to changes in the angle of attack, due to the effect of the wake. This dependence of time history [7] is the essence of unsteady aerodynamics and in this example is related to the Wagner effect [8], possibly relevant to insect flight [9]. The coefficient M_α will not be a constant, but a function of time according to the linear integral equation:

$$M_\alpha(t) = M_\alpha^\infty\Big(K(t)\alpha(t_0) + \int_{t_0}^{t} K(t-\tau)\alpha'(\tau)d\tau\Big), \tag{10}$$

where M_α^∞ is the steady value. Assuming that the kernel K is known, substitution of (10) to (9) will result in an integro-differential equation and the analysis becomes involved. However, only the recent time history has significant influence, so it is feasible [10, 11] to approximate (10) as

$$M_\alpha(t) \approx M_\alpha\alpha(t) + M_{\dot\alpha}\dot\alpha(t), \tag{11}$$

where both coefficients M_α and $M_{\dot\alpha}$ are constant.

Inclusion of approximate unsteady effects, as in (11), leads to representing X, Y, Z in (1)–(3) and L, M, N in (4)–(6) as linear combinations of $\boldsymbol{\delta x}$ and $\boldsymbol{\delta \dot{x}}$, so that (9) becomes

$$\boldsymbol{E}\boldsymbol{\delta \dot{x}} = \boldsymbol{A}_c\boldsymbol{\delta x}. \tag{12}$$

Here the matrix $\boldsymbol{E}$ has constant entries and is invertible, so that both sides of (12) can be multiplied by $\boldsymbol{E}^{-1}$ and the result is mathematically no more involved than (9).

Formulae (10) and (11) are valid for small values of α. In severe manoeuvres [12] the integral equation corresponding to (10) is nonlinear, so that M_α and $M_{\dot\alpha}$ in (11) depend on α and $\dot\alpha$,

$$\begin{aligned} M_\alpha &= M_\alpha(\alpha, \dot\alpha) \\ M_{\dot\alpha} &= M_{\dot\alpha}(\alpha, \dot\alpha), \end{aligned} \tag{13}$$

rather than being constant. This makes (9) quasi-linear [13]

$$\boldsymbol{\delta \dot{x}} = \boldsymbol{A}_c(\boldsymbol{\delta x}, \boldsymbol{\delta \dot{x}})\boldsymbol{\delta x}, \tag{14}$$

i.e. the entries of the matrix $\boldsymbol{A}_c$ are no longer constant, but depend on the perturbation $\boldsymbol{\delta x}$ and its derivative $\boldsymbol{\delta \dot{x}}$. Unlike for (12), it may not be possible to express (14) with $\boldsymbol{\delta \dot{x}}$ on one side of the equation. The resulting implicit, nonlinear differential equation is not easy to analyse and use.

An attractive alternative is to combine the fully nonlinear description (8) with an exhaustive collection of its linear approximations (12), so that both nonlinear and unsteady aspects are captured in a mathematically tractable way. This alternative is realised by bifurcation analysis, a state-of-the-art approach to nonlinear aircraft dynamics [14]. The validity and usefulness of this approach has been extensively verified over the last twenty years on real data from manoeuvring fighter aircraft: the F-8 [15, 16], the F-4 [17, 18], the F-14 [19], the F-16 [20] and the research configurations of their modern successors: the F-18/HARV [21, 22], HIRM [23, 24].

The first step in bifurcation analysis [17, 19] is to calculate all the steady states of the system by setting $\boldsymbol{f}_c(\boldsymbol{x}, t) \equiv 0$ in (8). Then, local stability of each steady state is investigated by examining the eigenvalues of the matrix $\boldsymbol{E}^{-1}\boldsymbol{A}_c$ in (12): negative eigenvalues mean that the steady state is stable, positive that it is unstable. Transition from a stable to unstable steady state (or *vice versa*) means that some eigenvalues will continuously pass through zero. Changes in the stability of a steady state are manifestations of nonlinearity and lead to qualitative changes of dynamic behaviour which are called bifurcations. Such qualitative changes can be analysed by the well-developed mathematics of bifurcation theory [25, 26, 27], together with the associated numerical and software tools [28, 29].

The essence of the external modelling approach to insect flight dynamics is: (i) to obtain empirically a nonlinear, unsteady model (8) with dynamic stability derivatives (13), and (ii) apply bifurcation analysis to the resulting model.

2.3 Internal modelling: Sensor rich feedback control

Insect flight dynamics are complex [9, 30] and are modelled by nonlinear differential equations. Their real-time solution requires considerable computing resources, while

flight control commands probably originate from a few hundred neurons. Although individual neurons do not function in the same way as an on-off (binary) transistor, making it difficult to translate number of neurons directly into computing power, it is reasonable to assume that these few neurons give the fly rather little processing power. At the very least, it is unlikely that insects solve differential equations by general purpose computation as the digital computers of aircraft do in real-time.

On the other hand, a typical insect brain, such as that of the blowfly *Calliphora* [31], receives sensory inputs from ca 80,000 receptor axons and has ca 338,000 neurons. The sensor rich character of this architecture is reflected by the fact that 98% of the neurons are used for sensory processing, as opposed to general purpose computation as in digital microprocessors. In contrast, there are only about a dozen of wing muscles, so the system is not actuator rich. For flying, the visual system is of critical importance [32, 33, 34], as are some mechanical sensors including antennae and wind-sensitive hairs. Two-winged flies, or Diptera, also have rotation sensors, called halteres [35, 36]. Most of the neural processing is devoted to vision and the insect's perception of the optic flow generated by flight is key to understanding its flight dynamics.

The fly's compound (made of ommatidia) eyes allow it to survey essentially the whole of the surrounding space, i.e. the full 4π steradians of the sphere on which the space is projected [37]. Further, the ommatidia outputs are processed locally by elementary motion detectors (EMDs). The EMD signals are then integrated by tangential neurons [38] to form a global vector field representing the relative motion of the insect with respect to its surroundings. This integration is done by at least thirteen tangential neurons [37] and each tangential neuron represents half (2π steradians) of the global vector field. Each tangential neuron responds to all kinds of optic flows, but is most sensitive to the flow corresponding to a specific, or preferred, direction of the insect's motion, see Figure 2.

A flying insect does not integrate its equations of motion numerically (8) in real time, but what it does must be equivalent to having solutions of such equations. The main hypothesis of the sensor rich feedback control concept [39] is that a fly (or locust) knows the solutions from optic flow measurement afforded by its vision system. There are three aspects of the theory.

Firstly, the vector field $\boldsymbol{\phi}$ of the optic flow is an encoded representation of the vector field $\boldsymbol{\mu}$ of the dynamics of relative motion of the insect with respect to its patterned surroundings. The vector field $\boldsymbol{\phi}$ of the optic flow, as in Figure 3, is a depiction of the kinematics of the relative motion. What must be inferred from $\boldsymbol{\phi}$ is the dynamics of this motion, i.e. the vector field $\boldsymbol{\mu}$, and thence the vector field $\boldsymbol{f}_c$ of the absolute dynamics (8). For a given trajectory and control law $\boldsymbol{f}_c$ is the same, while $\boldsymbol{\mu}$ will depend on the surroundings.

Secondly, the vector fields considered are formed on a sphere, a situation for which an extensive theory [40, 41] is available. The two-dimensional sphere has particularly convenient global (topological) properties leading to powerful results. For example, every smooth vector field must have at least one point at which the corresponding vector vanishes [42]; two such singular points can be seen in Figure 3. These are elementary manifestations of the well-developed [43] theory of the (singularity) index of vector fields, which is particularly powerful [44, 45] for the two-dimensional sphere. It is possible that the fly needs only to detect singularities to infer several global properties

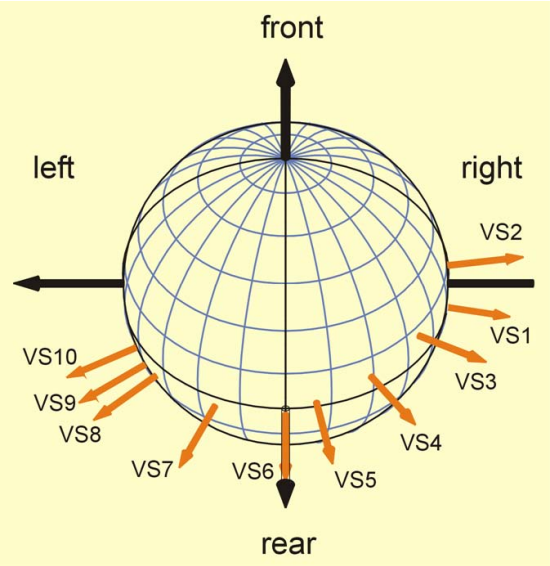

Figure 2: Preferred rotation axes of VS tangential neurons [37], i.e. directions of insect's motion generating the optic flow to which a given VS neuron's response is best matched.

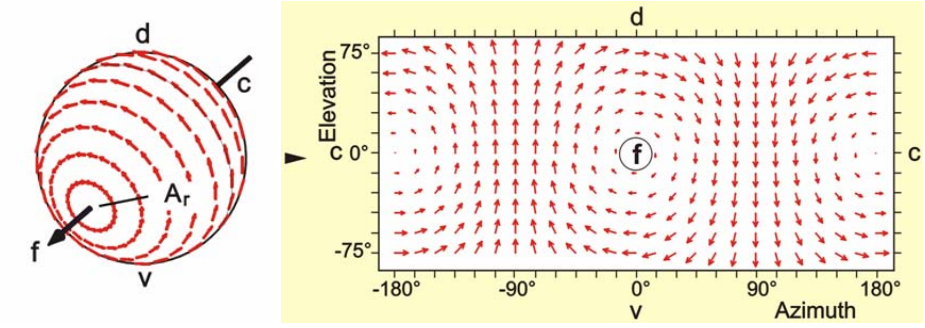

Figure 3: Optic flow $\boldsymbol{\phi}$ representation of the vector field $\boldsymbol{\mu}$ of the relative motion of the fly with respect to its surroundings when rotating along the long axis of its body (f frontal, c caudal, d dorsal, v ventral, A_r axis of rotation); from [38].

of its flight dynamics.

Thirdly, the insect can, through its tangential neurons [37], simultaneously measure overlapping patches of the global vector field, each patch covering at least a half-sphere. It is a more natural representation of a sphere than the Mercator projection of Figure 3 where two antipodal points are represented discontinuously as lines. It also enables forming a system of several second-order equations, so that recovering six degrees of freedom is possible. Moreover, tangential neurons are matched filters: they always respond to the insect's motion, but respond best (are tuned to) rotations or translations along certain directions in space, see Figure 2. This may allow resolution of geometric ambiguities in representing the absolute dynamics of the fly in the three-dimensional Cartesian space from their projection on a two-dimensional sphere. Also, the mutiple views of the vector field may allow its representation via orthogonal or even the Hodge decomposition [46]. Finally, since several overlapping patches (visual fields) are available simultaneously, a series of small (and thus easily controlled) adjustments are needed for the desired patterns of the vector field to be achieved.

In summary, sensor rich feedback control relies on extensive measurement, as opposed to heavy computation, of the quantities of interest. The visual system of the fly represents its motion relative to the environment through optic flow representation of the vector field involved. The underlying differential equations need not be integrated numerically, as their solutions are available through interpolation of the global representation of the relevant vector field. Also, this redundant representation may allow fine control with little computation.

The focus of the proposed internal modelling approach is understanding the relations between the vector fields: $\boldsymbol{\phi}$ of the optic flow, $\boldsymbol{\mu}$ of the dynamics of relative motion, and $\boldsymbol{f}_c$ of the dynamics of the absolute motion (external model).

2.4 Non-linear time-periodic models

In [1] we proposed and derived a semi-empirical nonlinear time periodic (NLTP) model of the longitudinal flight dynamics of desert locust, see equations (5.1)–(5.4) on page 209 of [1]. In that model nonlinearity comes from inertial and kinematic couplings, while the unsteady (and nonlinear) aerodynamics is represented as periodic input, since the force production is a result of cyclical wingbeat.

Mathematically, this can be interpreted as a nonlinear system forced by nonlinear oscillations and raises a few questions of theoretical and practical import. Some of these are considered in the discussion section of [1], especially §§6.5–6.6 between pages 218–220, where conjectures about (i) limit cycle control, (ii) orbital stability and (iii) asymptotically autonomous systems are proposed. Below we consider some new aspects of (i), see Section 2.5, and also point out some tools relevant to (iii), see Section 2.6.

The NLTP approach is analogous in some respects to the time-periodic models used to analyse helicopter flight dynamics in situations where the periodic rotor forces interact with the natural modes of the body (so-called 'air resonance' problems [47, 48, 49, 50]). However, whereas coupled rotor-fuselage models of helicopters have tended to use quasi-steady aerodynamic modelling [47, 49], the empirical measurements used

to parameterise our time-periodic model of locust flight automatically account for the periodic influence of unsteady aerodynamics.

The theoretical and empirical basis of the NLTP model is dealt with in full detail in the reprint of our paper [1] appended to this report.

2.5 Synchronisation

The NLTP model [1] is novel, especially in the context of insect flight dynamics, but at the same time belongs to the large subject of Nonlinear Oscillations. Interestingly, there are at least three issues here that are seldom considered together in the Theory of Oscillations, namely:

1. when will the solutions be oscillatory?
2. when will the solutions *not* be oscillatory?
3. how can 1 and/or 2 be effected by a limit cycle control scheme?

There are many mathematical results which throw light on each of these questions separately, but it does not seem immediately obvious how the disparate mathematical techniques involved could be used in an integrated way. An interesting alternative is to go back to the physical and engineering origins of nonlinear oscillations where an integrated approach was a necessity *per force*. This alternative goes under the name of "synchronisation", e.g. see [51], [52], [53]. There has been a resurgence of interest in the subject due to the recent interest in chaos, but this aspect is not relevant to insect flight dynamics.

Systems as diverse as coupled clocks, flashing fireflies, cardiac pacemakers, firing neurons, and applauding audiences exhibit a tendency to operate in synchrony, i.e. by tuning and retuning their nonlinear oscillations. A precise definition of synchronisation in general is usually either too restrictive or too broad, but includes phase locking and frequency entrainment, periodic forcing or interaction of periodic oscillators and noise-influenced synchronisation. In all cases, the dynamical system splits into subsystems that affect each other by interaction, and the problem is to understand how the interaction determines the dynamics of the system as a whole. In the context of the NLTP model of insect flight dynamics the phenomena of interest are:

1. synchronisation of a periodic oscillator by external force
2. suppression of oscillations

As for 1, this entails both phase and frequency locking and can be achieved by applying a weak force, i.e. a *small* amplitude oscillation. In particular, entrainment can be effected by a weak pulse train. This seems a plausible scheme for the direct muscles actuating insect wings for flight control. Indeed, it is compatible with the limit cycle control hypothesis and also consistent with the asymptotically autonomous character of the control proposed in [1]. This can be explained as follows. The wing-thorax system of the insect oscillates with frequency ω_0 and the wings are controlled by direct muscles which are much smaller (weaker) than the thoracic muscles. If the direct

muscles act on the wings with a weak, periodic force (amplitude ϵ and frequency ω), they can retune the wing-thorax system to a new oscillating frequency wing-thorax Ω. In general, this new frequency is different from the old one and the forcing one as well, $\Omega \neq \omega_0$ and $\Omega \neq \omega$. The larger the detuning $\omega_0 - \omega$, the larger the amplitude ϵ must be to achieve this new Ω. This can be captured precisely and illustrated graphically by the entrainment region in the ω-ϵ plane through the so-called Arnol'd tongues (triangle-like regions with vertex at $\omega = \omega_0$, widening upwards for increasing values of ϵ). Also worth noting, is that this theory is still applicable under random fluctuations, when frequency diffusion is observed, a phenomenon consistent with a range of flapping frequencies described in §4.2 of [1].

As for 2, a weak impulse train can be used to suppress oscillations. This means forcing the system off a limit cycle to a neighbouring point equilibrium, in effect a controlled Hopf bifurcation (see our previous Progress Report of November 2004). Indeed, in both synchronisation and suppression, the Poincaré map (stroboscopic observation of nonlinear oscillations) of bifurcation analysis is a tool of choice.

Finally, it is worth mentioning that synchronisation issues are related to the observer theory of nonlinear control [53]. The link is through the Reconstruction Theorem of bifurcation analysis [54] which is a result systematising reconstruction of attractors from data, hence providing a link between nonlinear theory and practical experiment.

2.6 Limiting equations

It was argued in §6.4 of [1] that, while the NLTP model is explicitly time-varying, it must—in effect—be asymptotically autonomous (time-invariant). As mentioned in the paper, the idea goes back to Markus [55], but there has been important progress in this area [56, 57] since his paper appeared in 1956. In particular, stability theory has been worked on with some success, e.g. see the appendix of [58]. More broadly, the method of limiting equations has emerged as a relevant technique [59].

The main idea can be illustrated beginning with a non-autonomous ordinary differential equation

$$\dot{\boldsymbol{x}} = \boldsymbol{f}(t, \boldsymbol{x}), \quad t \geq t_0, \tag{15}$$

where the right-hand side is defined for $\boldsymbol{x}$ in some open subset of $\mathbb{R}^n$. Suppose that there is a sequence $t_k \to \infty$ such that $\boldsymbol{f}(t + t_k, \boldsymbol{x}) \to \boldsymbol{g}(t, \boldsymbol{x})$ in the compact-open topology. Then

$$\dot{\boldsymbol{x}} = \boldsymbol{g}(t, \boldsymbol{x}) \tag{16}$$

is a limiting system of (15). Various properties of the solutions of (15), e.g., boundedness and stability, can be deduced if the class of limiting systems (16) satisfies appropriate conditions. Of particular interest is the case when the limiting equation is itself autonomous, i.e. the right-hand side g in (16) does not explicitly depend on time t, $g = g(x)$. For example,

$$\begin{aligned} \dot{x}_1 &= x_2 \\ \dot{x}_2 &= x_1 + x_2 + x_1 \sin\sqrt{t} \end{aligned} \tag{17}$$

has as its limiting equation

$$\dot{x}_1 = x_2$$

$$\dot{x}_2 \quad = \quad \mu x_1 + x_2, \tag{18}$$

where $\mu \in [0, 2]$. More interestingly,

$$\dot{\boldsymbol{x}} = \boldsymbol{g}(\boldsymbol{x}) + \boldsymbol{h}(t, \boldsymbol{x}) \tag{19}$$

is asymptotically autonomous if for every sequence $\boldsymbol{u}_k$ of functions $\boldsymbol{u}_k : [a, b] \to \mathbb{R}^n$, continuous on $[a, b]$ and converging to $\boldsymbol{u}_0$,

$$\int_a^b \boldsymbol{h}(t_k + s, \boldsymbol{u}_k(s))ds \to 0.$$

There are two kinds of results on stability. The first kind deduces stability properties of (15) from stability properties of (16) by constructing a Lyapunov function for (16). The second kind uses a scalar comparison equation for (15). It is assumed that the comparison equation admits a Lyapunov function. A main point is that a Lyapunov-type function is only assumed to exist for the comparison equation; on the other hand, the limiting comparison systems are assumed to have non-positive right-hand sides.

Finally, there are a few (but not many) results pertaining to the feedback control problem. Here the issue is whether a feedback control law designed for (16) will also work for (15). In general, this is a difficult question, but some results on stabilising control can be derived.

3 Experimental work

This section presents experimental aspects of the project. As was mentioned in Section 1, we decided at an early stage to develop an experimental apparatus capable of making the measurements required to parameterise the semi-empirical models described in Section 2 for forward flight as well as for hover. The rationale for tackling this more difficult problem at the outset was that it would be difficult later to adapt an apparatus designed for simulating hover so as to allow us to simulate forward flight in future work. The key challenge in simulating forward flight is to provide appropriate visual motion stimuli at the same time as providing an airflow of variable speed and incidence and a means of simulating the manoeuvres and body oscillations associated with natural free flight. The solution that we have developed is described in detail in Section 3.3 below, but we begin by discussing results from several other experimental setups that we have used in the course of developing this solution. We first discuss the results of experiments to measure "dynamic derivatives" for desert locusts (Section 3.1). We then recent work with free-flying *Eristalis* hoverflies (Section 3.2). Finally, we provide a detailed description of the new flight simulator (Section 3.3).

3.1 Dynamic stability/control derivatives of Desert Locusts

The experimental approach taken in [1] was to measure the instantaneous forces and moments generated by locusts tethered statically in a wind tunnel, and to represent the measured forces as time-periodic [1] fitted functions of speed and body angle.

This experimental approach was designed to be analogous to the classical engineering technique of measuring "stability derivatives" (see e.g. [60]), although it should be noted that the "derivatives" measured here represent the combined effects of passive stability and active control. Two major limitations of the experiments described in [30, 1] were that it was not possible to measure the effects of pitch rate damping (because the insect was tethered statically in the wind tunnel), and that the effects of pitch attitude and aerodynamic incidence were conflated (because adjusting the body angle of the insect changes its pitch attitude and aerodynamic incidence together). The latter means that derivatives measured with respect to changes in body angle were composite derivatives (see [60]), and it is therefore ambiguous how their effects should be represented in the linear system matrix or non-linear map of the forces. These experimental limitations are dealt with in detail in [1], a reprint of which is appended to this report.

The experiments described in this section of the report were designed to overcome the limitations of our earlier experimental work by: a) oscillating the locust in pitch to measure the pitch rate damping, and b) allowing the freestream incidence to be varied independently of the locust's pitch attitude. The aim of these experiments was to make quantitative predictions about the degree of visual feedback necessary to stabilise locust flight, and to this end we were interested in measuring the insect's response in the absence of visual stimuli. The experiments were therefore conducted in a blacked-out and darkened chamber. However, dim diffuse overhead lighting was provided to allow the ocelli (simple light detectors) to operate, while preventing the compound eyes from forming images. The exact light levels used were chosen to correspond to starlit nighttime conditions, under which locusts will often fly when on migration.

3.1.1 Methods

Desert locusts *Schistocerca gregaria* were first scrutinised for good physical condition (i.e. intact wings, appendages and antennae), and then selected on the basis of strong free flight ability. The subjects were mounted on a miniature 6-component force-moment balance via a mounting plate held in place by cyanoacrylate adhesive to the ventral surface of the thorax (natural frequency of the locust-balance system, ca. 560Hz). The insects were stimulated to fly in a jet of air of variable speed (0-5m/s) provided by a laminar blower, and would fly reliably, without stopping, for periods in excess of 2h. An infrared camcorder was used to monitor the locust's movements in order to check that it was flying consistently throughout the experiment.

The incidence of the airflow could be adjusted by tilting the blower (which was mounted on a pivoting frame) away from the horizontal. Flight conditions were totally dark, except for diffuse overhead lighting provided by an array of miniature DC tungsten bulbs run from two 1.5V batteries. The bulbs were suspended above a circular diffuser to remove any sharp contrasting edges from the locust's field of view, and were intended to provide the ocelli with the dorsoventral contrast necessary for flight stability, while preventing the compound eyes from seeing the fixity of the static surroundings.

The force balance was mounted on a cradle suspended about a transverse horizontal axis coincident with the insect's centre of mass. The cradle could be driven through a series of small amplitude pitch oscillations at frequencies up to 20Hz (just in excess of

wingbeat frequency, 19Hz) in order to simulate the small amplitude pitching oscillations expected to be experienced by locusts in flapping flight [1]. The dynamic forces and moments generated by the locust were sampled at 10kHz using an analogue to digital converter (Powerlab 16S/P), under the following flight conditions:

Pitch attitude series In these tests, force-moment measurements were taken over a 200s sampling period while the locust's body angle was varied in a slow (0.1Hz) oscillation from 15° to 2° in a horizontal flow of 4ms^{-1}.

Aerodynamic incidence series In these tests, force-moment measurements were taken over 6s sampling periods with the locust's body angle fixed at 9°, but with the angle of incidence of the oncoming 4ms^{-1} flow varied from $-7°$ to 5°, alternating positive and negative to avoid correlating blower angle with time of measurement.

Speed series In these tests, the body angle of the locust was held fixed at 9° in a horizontal flow. The speed of the blower was varied between 50% and 100% (approximately 2 to 5ms^{-1}), alternating speeds above and below the reference speed (70%, 4ms^{-1}) to avoid correlating speed with time of measurement.

Pitch oscillation series In these experiments the locust was oscillated between 13° and 5° at a range of frequencies (1, 2, 4, 6, 8, 10, 15, 20Hz), in a horizontal flow of 4ms^{-1}. The locust was also oscillated at its wingbeat frequency (ca 19Hz) as calculated from the earlier measurements on order to simulate the periodic pitch oscillations that locusts are expected to experience in free flight [1].

Calibration and weighing The inertial forces acting on the locust during the pitch rate tests were measured directly by repeating the pitch rate tests after the locust had been euthanised (by freezing) and set into a mid- downstroke posture using tiny amounts of cyanoacrylate adhesive. The locust was enclosed by a plastic container which had no contact with the force measurement apparatus, but was oscillated with the cradle. This method parallels an engineering technique commonly used to measure tare loads during dynamic wind tunnel testing. Following the experiments, the dead locust was weighed to determine the mass of each body segment, to allow calculation of the position of its centre of mass and of the moment of inertia about this point.

3.1.2 Results and analysis

At present, we have completed a time-invariant, but not yet time-periodic, analysis of the forces and moments. This is justified on the grounds that the results of the analysis predict that the time-invariant system is unstable in the absence of visual stimuli, and it is unlikely that the more involved NLTP analysis would show the system to be stable. On the other hand, the classical techniques of eigenvalue analysis permitted under a linear time-invariant (LTI) framework allow quick estimates to be made of the magnitude of damping that the vision-based control pathway would need to provide for the system to be stable. The time-invariant analysis used follows a method similar

to that described in [30] for the static measurements, but follows a slightly different method for the oscillation series, using the dynamic calibration to correct the measured forces. The details of this approach are not detailed further in the summary of the experiments provided here.

Fig. 3.1.2 plots the measured forces against the state variables for a single individual, typical of those from which measurements were taken. Forces measured in the speed and aerodynamic incidence series are time-averaged; forces measured in the oscillation series are left as instantaneous measurements and plotted against instantaneous pitch rate. Aerodynamic incidence, speed and pitch attitude derivatives were estimated from these graphs as the slopes of the least-squares linear regressions fitted to the data. Forces measured during the pitch attitude series were used to estimate the composite pitch attitude and aerodynamic incidence derivatives, from which we were able to estimate the pure pitch attitude derivatives by assuming that the composite derivatives were the linear sums of the pitch attitude and aerodynamic incidence derivatives.

The various derivatives were then used to populate the LTI system matrix $\boldsymbol{A}$, from which the stability of the LTI system

$$\dot{\boldsymbol{x}} = \boldsymbol{A}\boldsymbol{x} \tag{20}$$

could be determined. The LTI system was always found to be unstable, and we were therefore able to estimate the degree of visual feedback required to stabilise the system by assuming that visual feedback modifies the pitching moment derivative with respect to pitch attitude. This allowed is to determine the degree of feedback required to a) stabilise the system and b) provide critical damping of its oscillatory modes. This was done by iteratively varying the value of the component M_θ (rate of change in pitching moment with pitch atttitude) in $\boldsymbol{A}$ and recalculating the eigenvalues of $\boldsymbol{A}$ for each value of M_θ:

$$\boldsymbol{A} = \begin{bmatrix} X_U/m & X_\alpha/mu_e & X_q/m - w_e & -g\cos\theta_e \\ Z_U/m & Z_\alpha/mu_e & Z_q/m + u_e & -g\sin\theta_e \\ M_U/I_{yy} & M_\alpha/I_{yy}u_e & M_q/I_{yy} & M_\theta/I_{yy} \\ 0 & 0 & 1 & 0 \end{bmatrix} \tag{21}$$

Using this procedure, analogous to the graphical root locus plot technique [3], we were able to determine the critical values of M_θ for which a) the real parts of all of the eigenvalues became negative and b) the imaginary parts of all of the eigenvalues became zero.

In the case of the locust shown in Figs. 3.1.2, the model predicts that instantaneous pitch attitude changes detected by the visual system would need to feed into the pitching moment at a rate of $M_\theta = -1.3\text{mN m rad}^{-1}$ to provide stability and at a rate of $M_\theta = -1.6\text{mN m rad}^{-1}$ to provide critical damping of the short period mode. To provide some physical meaning to these otherwise rather abstract numbers, this is equivalent to the resultant aerodynamic force shifting ca. 1mm aft for every degree of positive pitch. Since the wing length of a desert locust is ca. 50mm, it is clear that this ought to be achievable with relatively small changes in, for example, the mean longitudinal position of the wings through the stroke.

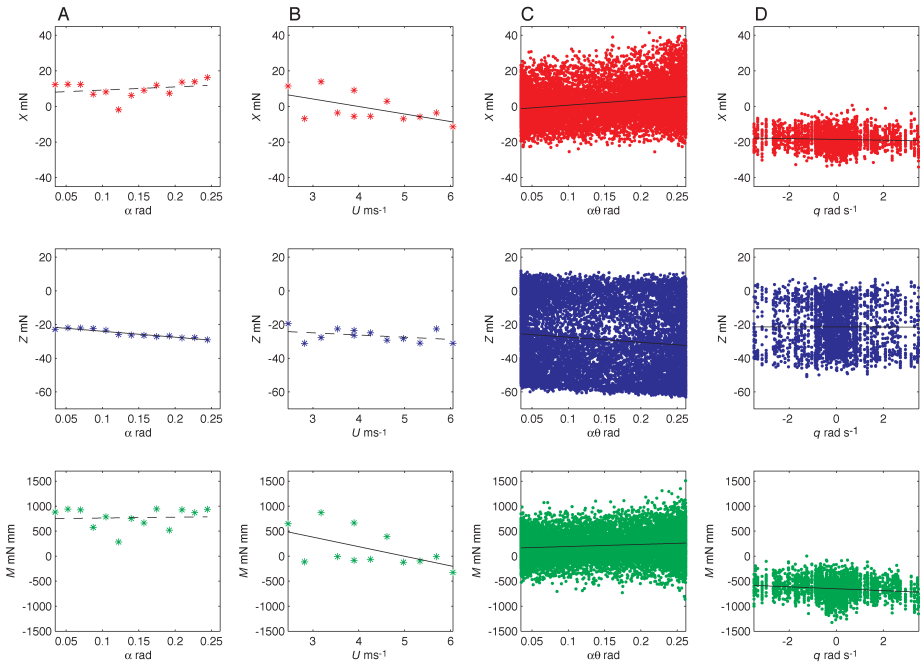

Figure 4: Graphs plotting the measured forces and moments against the state variables. A. Time-averaged forces from the aerodynamic incidence series against aerodynamic incidence. B. Time-averaged forces from the speed series against wind speed. C. Instantaneous forces from the pitch attitude (slow oscillation) series against pitch attitude, equal to aerodynamic incidence. D. Instantaneous forces from the pitch rate (fast oscillation) series against pitch rate. Plots of instantaneous forces plot 1 datapoint in every 100. The black lines are least-squares linear regressions fitted to the data; the line is solid if the slope is significantly different from zero ($p < 0.05$) and dashed otherwise. The slope of the regression line gives the value of the corresponding derivative, treated as zero if the slope was non-significant

3.1.3 Discussion

In general, these experiments show that the effect of varying aerodynamic incidence on its own differs from the effect of varying aerodynamic incidence and pitch attitude together in the desert locust. This result confirms that the use of composite derivatives in [30, 1] could lead to misleading results, as discussed in those papers, and argues for the need to assess their effects separately as we have done here. The graphs also confirm, as expected, that pitch rate has a significant effect on the forces and moments produced. It is therefore essential that experiments on insect flight control should measure pitch rate damping. Since the models developed using this incarnation of the flight simulator apparatus (i.e a dynamic rig and variable-incidence wind tunnel with no visual input) predict an LTI system that is unstable, we decided to go no further with the analysis and instead to proceed with the development of the full flight simulator apparatus described below. Aspects of the dynamic rig developed in the present set of experiments are exploited in the new flight simulator design.

3.2 Preliminary experiments with *Eristalis* hoverflies

Because an eventual goal of this work was to derive a flight dynamics model for *Eristalis* hoverflies, a key aspect of the experimental component of this study was to verify whether the frequency response of our existing force balance was sufficient to characterise the forces and moments generated by these insects, which have a wingbeat frequency (ca. 150Hz) an order of magnitude higher than that of the desert locust (ca. 20Hz). There are two distinct components to this question. The first is to determine what frequency response is necessary to characterise those frequency components of the flight forces and moments that impact upon the flight dynamics. The second is to determine whether the force balance frequency response is sufficient for this.

In the case of the desert locust, we were able to measure statistically significant harmonics of force production up to about the 8th harmonic of the fundamental wingbeat frequency [1]. However, the NLTP flight dynamics model in [1] predicts that only the fundamental frequency (19 Hz) is important in determining the flight dynamics: the higher harmonics of the wingbeat frequency that we measured are, in effect, low-pass filtered by the body dynamics. It is not possible to determine the effective cut-off frequency for the hoverfly body dynamics directly without deriving its full equations of motion, which in turn cannot be done without reliable measurements of the periodic forces, and we therefore took the approach of observing the hoverfly body kinematics directly during hovering flight using high-speed videography.

By making recordings of hovering *Eristalis* hoverflies using 4 high-speed digital video cameras recording at 4000fps, we were able to verify that the time-periodic forcing of the wingbeat is not manifested strongly in the body dynamics, as oscillations of the body at the wingbeat frequency are scarcely discernible, even in video of sufficient resolution to resolve individual hairs on the fly's abdomen. This implies that it may not be necessary to formulate the full time-periodic equations of motion in order to model the flight dynamics of *Eristalis* hoverflies realistically. This is in contrast to the situation for the larger desert locust, whose larger size and longer time constants mean that a time-periodic model is essential, as shown in [1]. Arguably, because MAVs

are likely to be closer in size to the locust than to the hoverfly, it is probable that a time-periodic modelling framework will be necessary for modelling flapping-MAV flight dynamics.

Because a time-periodic representation of the forces is probably unnecessary in modelling hoverfly flight dynamics, it follows that if we can record the fundamental frequency of the hoverfly wingbeat faithfully using our force balance, we may be confident that the frequency response of the balance is adequate to model hoverfly flight dynamics. The frequency response of the balance is almost 600Hz with a hoverfly attached, and this should therefore be more than sufficient to measure reliably force components at the fundamental frequency of the wingbeat (ca. 150Hz).

3.3 Flight simulator

The key experimental goal in our re-scoped and re-focussed study into experimental aspects of insect flight dynamics modelling was to develop an apparatus suitable for deriving flight dynamics models for any large insect, including desert locusts and *Eristalis* hoverflies. The solution that we have finally reached is illustrated in Fig. 5.

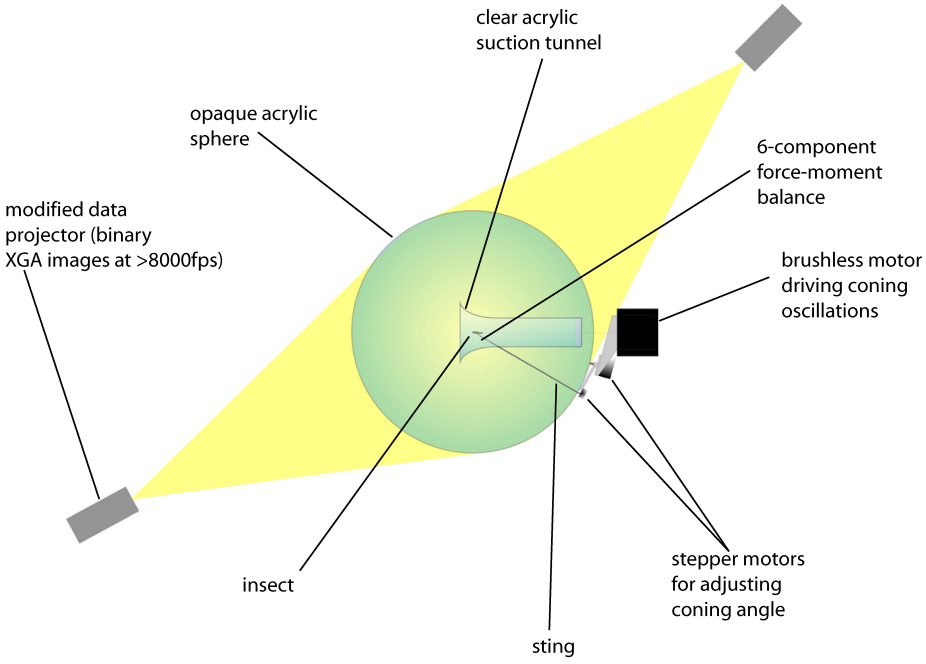

Figure 5: Schematic of the layout of the new flight simulator. See accompanying text for description.

Briefly, the insect is tethered to a 6-component force-moment balance mounted on a sting that can be oscillated in pitch, yaw or coning motions, similar to an arrangement formerly used by NASA in wind tunnel tests of high-performance aircraft. Airflow is

provided by an open-circuit cylindrical suction tunnel manufactured from clear cast acrylic, with clear plastic computer cooling fans used to induce an airflow quietly. The wind tunnel is transparent to allow the insect to see through its walls and onto the spherical projection screen that surrounds the whole apparatus. Two/three customised computer data projectors are used to back-project moving visual stimuli, comprising synchronised XGA binary images projected at frame rates in excess of 8kHz. This allows us to project moving images that will appear flicker-free and smooth, even to flies (which have an extremely fast visual system). The setup thereby provides an immersive visual environment for insects as well as airflow and inertial stimuli, and forms a complete virtual reality environment simulating natural free-flight.

A detailed description of the various components of this system is currently in preparation as a methods paper for publication in the biomechanics/neurophysiology literature. The flight simulator itself is the centrepiece of a recently-awarded BBSRC grant to GKT, in which flight dynamics models are to be developed for blowflies and locusts, and combined with recordings from certain visual processing neurons made by Dr Holger Krapp (Imperial College) and Prof. Simon Laughlin (Cambridge). This research will provide basic data needed to link internal and external models of flight dynamics of the kind discussed in Section 2.

References

[1] G. K. Taylor and R. Żbikowski. Nonlinear time-periodic models of the longitudinal flight dynamics of desert locusts *Schistocerca gregaria*. *Journal of the Royal Society Interface*, 2(3):197–221, 2005.

[2] J. Roskam. *Airplane Flight Dynamics and Automatic Flight Controls. Part I*. DARcorporation, Lawrence, KS, 1995.

[3] B. Etkin and L. D. Reid. *Dynamics of Flight. Stability and Control*. Wiley, New York, Third edition, 1996.

[4] V. A. Yakubovich and V. M. Starzhinskii. *Linear Differential Equations with Periodic Coefficients*, volume 1. Wiley, New York, 1975.

[5] K. J. Orlik-Rückemann. Aerodynamic aspects of aircraft dynamics at high angles of attack. *Journal of Aircraft*, 20(9):737–752, 1983.

[6] G. J. Hancock. *An Introduction to the Flight Dynamics of Rigid Aeroplanes*. Ellis Horwood, New York, 1995.

[7] M. Tobak and L. B. Schiff. The role of time-history effects in the formulation of the aerodynamics of aircraft dynamics. In *Dynamic Stability Parameters*, volume 235 of *AGARD Conference Proceedings*, pages 26.1–26.10. 1978.

[8] H. Wagner. Über die Entstehung des dynamischen Auftriebes von Tragflügeln. *Zeitschrift für Angewandte Mathematik und Mechanik*, 5(1):17–35, 1925.

[9] R. Żbikowski. On aerodynamic modelling of an insect-like flapping wing in hover for micro air vehicles. *Philosophical Transactions of the Royal Society of London (Series A: Mathematical, Physical and Engineering Sciences)*, 360(1791):273–290, 2002.

[10] M. Tobak, G. T. Chapman, and L. B. Schiff. Mathematical modeling of the aerodynamic characteristics in flight dynamics. NASA Technical Memorandum 85880, National Aeronautics and Space Administration, 1984.

[11] H. H. B. M. Thomas. Some thoughts on mathematical models for flight dynamics. *Aeronautical Journal*, 88(875):169–178, 1984.

[12] J. E. McCune, C. G. Lam, and M. T. Scott. Nonlinear aerodynamics of two-dimensional airfoils in severe maneuver. *AIAA Journal*, 28(3):385–393, 1990.

[13] A. Tsourdos, R. Żbikowski, and B. A. White. Robust autopilot for a quasi-linear parameter-varying missile model. *Journal of Guidance, Control, and Dynamics*, 24(2):287–295, 2001.

[14] M. G. Goman, G. I. Zagainov, and A. V. Khramtsovsky. Application of bifurcation methods to nonlinear flight dynamics problems. *Progress in Aerospace Sciences*, 33(9–10):539–586, 1997.

[15] D.-C. Liaw and C.-C. Song. Analysis of longitudinal flight dynamics: A bifurcation-theoretic approach. *Journal of Guidance, Control, and Dynamics*, 24(1):109–116, 2001.

[16] D.-C. Liaw, C.-C. Song, Y.-W. Liang, and W.-C. Chung. Two-parameter bifurcation analysis of longitudinal flight dynamics. *IEEE Transactions on Aerospace and Electronic Systems*, 39(3):1103–1112, 2003.

[17] J. V. Carroll and R. K. Mehra. Bifurcation analysis of nonlinear aircraft dynamics. *Journal of Guidance, Control, and Dynamics*, 5(5):529–536, 1982.

[18] M. H. Lowenberg and A. R. Champneys. Shil'nikov homoclinic dynamics and the escape from roll autorotation in an F-4 model. *Philosophical Transactions of the Royal Society of London (Series A: Mathematical, Physical and Engineering Sciences)*, 356(1745):2241–2256, 1998.

[19] C. C. Jahnke and F. E. C. Culick. Application of bifurcation theory to the high-angle-of-attack dynamics of the F-14. *Journal of Aircraft*, 31(1):26–34, 1994.

[20] G. Avanzini and G. de Matteis. Bifurcation analysis of a highly augmented aircraft model. *Journal of Guidance, Control, and Dynamics*, 20(4):754–759, 1997.

[21] P. Gránásy and P. G. Thomasson. Non-linear flight dynamics at high angles-of-attack. *Aeronautical Journal*, 102(1016):337–343, 1998.

[22] N. K. Sinha. Application of bifurcation methods to F-18/HARV open-loop dynamics in landing configurations. *Defence Science Journal*, 52(2):103–115, 2002.

[23] Y. Patel and D. Littleboy. Piloted simulation tools for aircraft departure analysis. *Philosophical Transactions of the Royal Society of London (Series A: Mathematical, Physical and Engineering Sciences)*, 356(1745):2203–2221, 1998.

[24] M. H. Lowenberg and Y. Patel. Use of bifurcation diagrams in piloted test procedures. *Aeronautical Journal*, 104(1035):225–235, 2000.

[25] S.-N. Chow and J. K. Hale. *Methods of Bifurcation Theory*. Springer, New York, 1982.

[26] V. I. Arnol'd, V. S. Afrajmovich, Yu. S. Il'yashenko, and L. P. Shil'nikov. *Bifurcation Theory and Catastrophe Theory*. Springer, Berlin, 1999.

[27] M. Demazure. *Bifurcations and Catastrophes. Geometry of Solutions to Nonlinear Problems*. Springer, Berlin, 2000.

[28] E. L. Allgower and K. Georg. *Numerical Continuation Methods. An Introduction*. Springer, Berlin, 1990.

[29] W. J. F. Govaerts. *Numerical Methods for Bifurcations of Dynamical Equlibria*. SIAM, Philadelphia, 2000.

[30] G. K. Taylor and A. L. R. Thomas. Dynamic flight stability in the desert locust *Schistocerca gregaria*. *Journal of Experimental Biology*, 206(16):2803–2829, 2003.

[31] N. J. Strausfeld. *Atlas of An Insect Brain*. Springer, Berlin and New York, 1976.

[32] M. H. Dickinson. Linear and nonlinear encoding properties of an identified mechanoreceptor of the fly wing measured with mechanical noise stimuli. *Journal of Experimental Biology*, 151:219–244, 1990.

[33] M. H. Dickinson. Comparison of encoding properties of campaniform sensilla of the fly wing. *Journal of Experimental Biology*, 151:245–261, 1990.

[34] T. A. Keil. Functional morphology of insect mechnoreceptors. *Microscopy Research and Technique*, 39(6):506–531, 1997.

[35] G. Nalbach. The halteres of the blowfly *calliphora*. I. Kinematics and dynamics. *Journal of Comparative Physiology A*, 173(3):293–300, 1993.

[36] G. Nalbach and R. Hegstenberg. The halteres of the blowfly *calliphora*. II. Three-dimensional organization of compensatory reactions to real and simulated rotations. *Journal of Comparative Physiology A*, 175(6):695–708, 1994.

[37] H. G. Krapp. Neuronal matched filters for optic flow processing in flying insects. In M. Lappe, editor, *Neuronal processing of optic flow*, pages 93–120, San Diego, CA, 2000. Academic Press.

[38] H. G. Krapp and R. Hegstenberg. Estimation of self-motion by optic flow processing in single visual interneurons. *Nature*, 384(6608):463–466, 1986.

[39] R. Żbikowski. Sensor rich feedback control. *IEEE Instrumentation & Measurement Magazine*, 7(3):19–26, 2004.

[40] C. Godbillon. *Dynamical Systems on Surfaces*. Springer, Berlin, 1983.

[41] V. I. Arnol'd. *Ordinary Differential Equations*. Springer, Berlin, 1992.

[42] M. Eisenberg and R. Guy. A proof of the hairy ball theorem. *American Mathematical Monthly*, 86(7):572–574, 1979.

[43] D. H. Gottlieb. Vector fields and classical theorems of topology. *Rendiconti del Seminario Matematico e Fisico di Milano*, 60:193–203, 1990.

[44] J. Milnor. The characteristics of a vector field on the two-sphere. *Annals of Mathematics*, 58(2):253–257, 1953.

[45] J. F. Adams. Vector fields on spheres. *Annals of Mathematics*, 75(3):603–632, 1962.

[46] J. Cantarella, D. DeTurck, and H. Gluck. Vector calculus and the topology of domains in 3-space. *American Mathematical Monthly*, 109(5):409–442, 2002.

[47] W. Warmbrodt and P. P. Friedmann. Formulation of coupled rotor/fuselage equations of motion. *Vertica*, 3:245–271, 1979.

[48] P. P. Friedmann. Formulation and solution of rotary-wing aeroelastic stability and response problems. *Vertica*, 7(2):101–141, 1983.

[49] M. D. Takahashi and P. P. Friedmann. Active control of helicopter air resonance in hover and forward flight. AIAA Paper 1988-2407, AIAA, 1988.

[50] P. P. Friedmann. Helicopter rotor dynamics and aeroelasticity. *Vertica*, 14(1):101–121, 1990.

[51] A. Pikovsky, M. Rosenblum, and J. Kurths. *Sunchronization. A universal concept in onlinear sciences*. Cambridge University Press, Cambridge, England, 2001.

[52] A. L. Fradkov and A. Yu. Pogromsky. *Introduction to control of oscillations and chaos*. World Scinetific, Singapore, 1998.

[53] H. J. C. Huijberts and H. Nijmeijer. An observer view on synchronization. In A. Isidori, F. Lamnabhi-Lagarrigue, and W. Respondek, editors, *Nonlinear Control in the Year 2000*, volume 1. Springer-Verlag, 2001.

[54] T. Sauer, J. A. Yorke, and M. Casdagli. Embedology. *Journal of Statistical Physics*, 65(3/4):579–616, 1991.

[55] L. Markus. Asymptotically autonomous differential equations. In S. Lefschetz, editor, *Contributions to the theory of nonlinear oscillations*, volume 3, pages 17–29. Princeton University Press, 1956.

[56] A. Strauss and J. A. Yorke. On asymptotically autonomous differential equations. *Mathematical Systems Theory*, 1(2):175–182, 1967.

[57] Y. Wu. Oscillation via limiting equations. *Nonlinear Analysis, Theory, Methods & Applications*, 25(1):89–102, 1995.

[58] J. P. LaSalle. *The Stability of Dynamical Systems*. SIAM, Philadelphia, PA, 1976. (With Appendix "Limiting Equations and Stability of Nonautonomous Ordinary Differential Equations" by Z. Artstein).

[59] J. Kato, A. A. Martynyuk, and A. A. Shestakov. *Stability of Motion of Nonautonomous Systems (Method of Limiting Equations)*. Gordon and Breach Publishers, Luxembourg, 1996.

[60] B. Etkin. *Dynamics of atmospheric flight*. John Wiley and Sons, Inc., New York, 1972.